

SMART: Shot-Aware Multimodal Video Moment Retrieval with Audio-Enhanced MLLM

An Yu, Weiheng Lu, Jian Li, Zhenfei Zhang, Yunhang Shen, Felix X.-F. Ye, Ming-Ching Chang

arXiv:2511.14143v1 [cs.CV] 18 Nov 2025

Abstract—Video Moment Retrieval is a task in video understanding that aims to localize a specific temporal segment in an untrimmed video based on a natural language query. Despite recent progress in moment retrieval from videos using both traditional techniques and Multimodal Large Language Models (MLLM), most existing methods still rely on coarse temporal understanding and a single visual modality, limiting performance on complex videos. To address this, we introduce Shot-aware Multimodal Audio-enhanced Retrieval of Temporal Segments (SMART), an MLLM-based framework that integrates audio cues and leverages shot-level temporal structure. SMART enriches multimodal representations by combining audio and visual features while applying Shot-aware Token Compression, which selectively retains high-information tokens within each shot to reduce redundancy and preserve fine-grained temporal details. We also refine prompt design to better utilize audio-visual cues. Evaluations on Charades-STA and QVHighlights show that SMART achieves significant improvements over state-of-the-art methods, including a 1.61% increase in R1@0.5 and 2.59% gain in R1@0.7 on Charades-STA.

Index Terms—Video Moment Retrieval, Temporal Localization, Audio-Visual Representation Learning, Shot-aware Token Compression, Shot Boundary Detection, Temporal Reasoning, Multimodal Large Language Models (MLLM), Video Understanding.

I. INTRODUCTION

WITH the rapid growth of video content shared and created on the internet and social media, the ability to efficiently analyze such content has become increasingly important. One key task in this domain is **moment retrieval**—the process of identifying the specific temporal segment within a video that best corresponds to a given natural language query. This task is fundamental to a wide range of applications, including video summarization, content recommendation, security surveillance, and event localization. It has emerged as a prominent area of research due to its practical importance and inherent complexity.

Current moment retrieval methods can be broadly categorized into two main classes: traditional approaches [4], [9], [8], [58], [59] and approaches that leverage Multimodal Large Language Models (MLLM) [46], [47]. As shown in Figure 1a,

An Yu is with the Department of Computer Science, University at Albany - SUNY, Albany, NY 12222, USA.

Weiheng Lu is with the School of Software & Microelectronics, Peking University, Haidian District, Beijing, China, 100871.

Jian Li is with Nanjing University, Nanjing, Jiangsu, China, 210093.

Zhenfei Zhang is with the Department of Computer Science, University at Albany - SUNY, Albany, NY 12222, USA.

Yunhang Shen is with Xiamen University, Xiamen, Fujian, China, 361005.

Felix X.-F. Ye is with the Department of Mathematics and Statistics, University at Albany - SUNY, Albany, NY 12222, USA.

Ming-Ching Chang is with the Department of Computer Science, University at Albany - SUNY, Albany, NY 12222, USA.

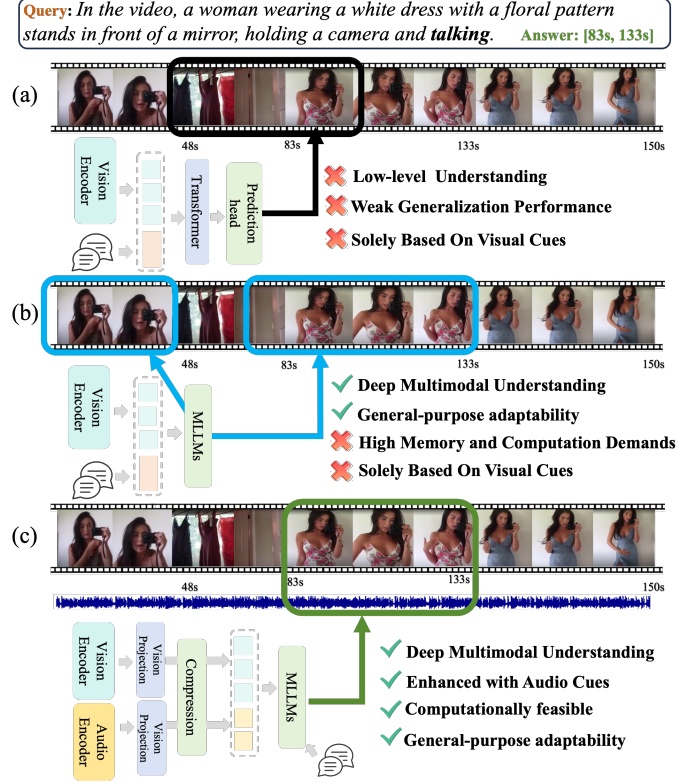


Fig. 1. Overview: (a) Traditional models rely on low-level visual features and generalize poorly. (b) MLLM-based models improve semantic understanding but ignore audio and incur high computational cost. (c) Our SMART model integrates audio and shot-coherent token compression for efficient, accurate, and generalizable multimodal moment retrieval.

traditional approaches typically adopt Transformer-based architectures with task-specific prediction heads. These methods often rely on low-level visual features and are tailored to specific tasks, which limits their ability to generalize and capture high-level semantics. In contrast, recent studies [49], [48], [18], [10], [57] have explored the use of MLLM to enhance semantic understanding for moment retrieval tasks. However, as illustrated in Figure 1b, these methods typically rely solely on visual information, overlooking the audio modality, which is crucial for capturing the full context of natural videos. For example, retrieving the moment for the query “*a woman is holding a camera and talking*” requires not only visual identification but also speech detection. Similarly, the sound of a siren is often key to identifying moments involving passing vehicles. Without audio, models risk misalignment between the natural language query and the correct video segment, as they rely solely on visual information to interpret temporal context. This unimodal assumption poses challenges,

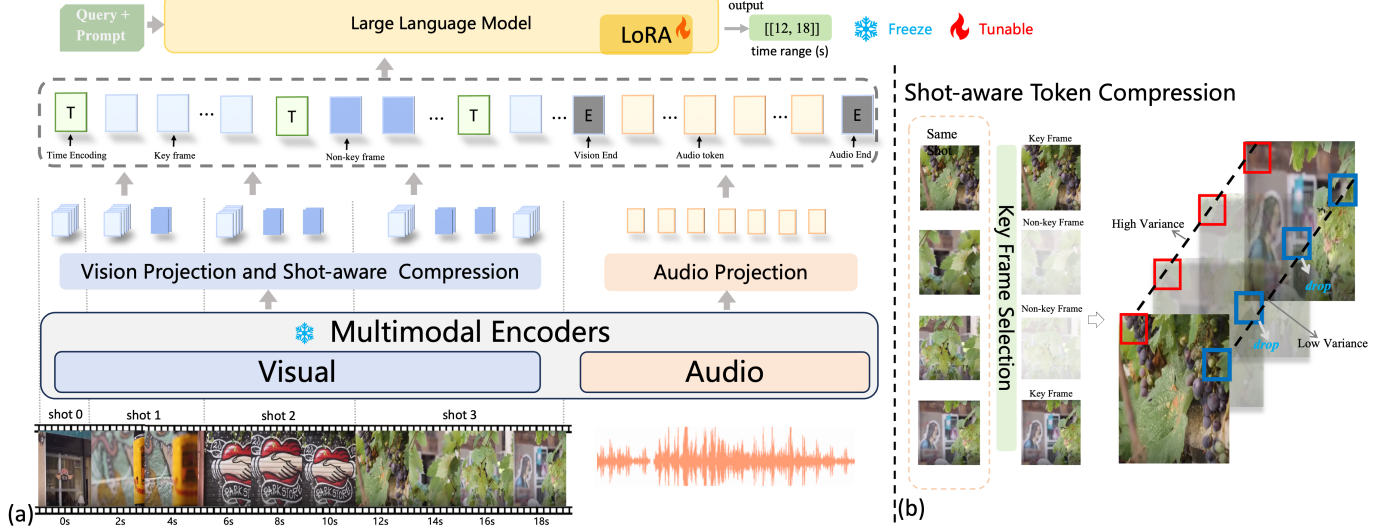


Fig. 2. The **Shot-aware Multimodal Audio-enhanced Retrieval of Temporal Segments (SMART) architecture**: (a) The SMART pipeline integrates a pretrained MLLM with frozen visual and audio encoders and a lightweight LoRA-tuned LLM to predict temporal segments relevant to a query. Visual and audio features are projected, temporally encoded, and concatenated into a unified multimodal prompt, with shot-aware token compression applied for efficiency. (b) The Shot-aware Token Compression (STC, detailed in Fig. 3) operates in two stages: frames are first classified into key and non-key frames based on inter-frame differences; then, token-wise variance within each shot is analyzed. High-variance tokens (red), representing dynamic content, are retained, while low-variance tokens (blue) from non-key frames are discarded to remove redundancy while preserving essential cues.

especially when temporal grounding depends on acoustic cues or joint audio-visual signals.

LLMs often face challenges when handling long input sequences, which restricts the amount of video content they can effectively process and leads to high memory and computational demands. As a result, they may fail to capture the complete and nuanced temporal context spread across extended video sequences, which is essential for accurately identifying and retrieving the segments that align closely with a given natural language query. The inefficiency in handling long sequences also poses a major scalability challenge, especially in real-world applications where videos are lengthy and complex. These constraints reduce their capacity to capture rich, multimodal temporal context, thus limiting their effectiveness in tasks that require precise and robust video understanding and moment retrieval.

To address these limitations in generalizability and scalability for real-world moment retrieval, we propose **Shot-aware and Multimodal Audio-enhanced Retrieval of Temporal Segments (SMART)**, a novel MLLM-based framework illustrated in Figure 1c. SMART integrates audio information and employs a dual-branch encoder to jointly process video and audio inputs, enriching multimodal representations and enabling more comprehensive temporal understanding. To reduce the computational cost of long input sequences, we introduce **Shot-aware Token Compression (STC)** that compresses redundant frame tokens within each shot. By computing token-level variance across frames using Q-Former outputs, it identifies and retains key tokens while discarding redundant ones. This compression preserves semantic richness and fine-grained temporal cues, allowing SMART to process longer video sequences efficiently without losing detail. The complete pipeline is shown in Figure 2.

We conducted extensive experiments on two widely

used benchmark datasets, Charades-STA [1] and QVHighlight [4], which are specifically designed for multimodal moment retrieval task. Experimental results demonstrate that SMART consistently outperforms state-of-the-art methods by effectively leveraging multimodal cues and modeling fine-grained temporal structures through shot-aware token compression. On the Charades-STA and QVHighlights datasets, SMART achieves notable performance gains over strong baselines—including LLaVA-MR and Mr.BLIP—with improvements of +1.56% R1@0.5 on QVHighlights and +1.61% R1@0.5 and +2.59% R1@0.7 on Charades-STA.

Contributions of this paper are summarized as follows:

- We present a novel MLLM-based framework that integrates both visual and audio modalities to improve multimodal representation learning and enhance semantic understanding in moment retrieval.
- We propose a Shot-aware Token Compression strategy that eliminates redundant tokens within each shot to improve computational efficiency while preserving key temporal information.
- We conduct comprehensive evaluations on benchmark datasets, demonstrating substantial improvements over existing state-of-the-art methods.

II. RELATED WORKS

A. Moment Retrieval

Moment Retrieval (MR) aims to localize the video segment that best corresponds to a natural language query, making it a fundamental task in video understanding. Early MR methods, such as TALL [1], relied on sliding windows for temporal localization, but their high computational cost motivated the development of more efficient approaches, including attention-based boundary prediction [20]. Subsequent models, including

Semantic Conditioned Dynamic Modulation [21] and the Moment Alignment Network (MAN) [22], introduced dynamic video–text alignment through graph-based mechanisms.

In the related task of Temporal Action Detection (TAD), early approaches employed multi-stage CNNs [52] and Temporal Convolutional Networks (TCNs)[23], which later evolved into more structured frameworks such as Structured Segment Networks (SSN) [24] and Graph Convolutional Networks (GCNs) [25]. More recently, Transformer-based architectures, including ActionFormer [26] and Unified Multi-Modal Transformers (UMT) [27], have significantly advanced temporal modeling and multimodal integration.

Despite these advances, most existing approaches remain constrained by annotation bias and task-specific or rigid prediction head designs, which hinder generalization. To address these challenges, SMART leverages Multimodal Large Language Models (MLLMs) to achieve richer cross-modal understanding, offering both greater flexibility and improved performance.

B. Multimodal Large Language Models

Building on the success of Large Language Models (LLMs), Multimodal Large Language Models (MLLMs) have been developed to enhance cross-modal understanding by integrating visual, auditory, and textual information. Several approaches [30], [31], [32], [33] extend LLMs with additional components such as gated cross-attention modules or adapter layers to process multimodal inputs. Others [34], [35], [36] adopt projection layers or Q-Formers to map visual encoder outputs into the LLM embedding space.

Video-oriented LLMs [37], [40], [39], [38], [53] further extend these designs to temporal data, typically employing projection layers or Q-Formers to encode video tokens. Recent efforts such as Mr. BLIP [10] and LLaVA-MR [18] have achieved state-of-the-art performance in moment retrieval, benefiting from MLLMs’ enhanced semantic alignment and improved cross-modal generalization. Meanwhile, other works [41], [42], [43] incorporate audio as an additional modality, but often suffer from redundancy and inefficiency caused by the absence of effective token compression mechanisms.

To address these limitations, our proposed SMART integrates audio in a shot-aware token compression mechanism that maintains temporal coherence. This design enables fine-grained temporal reasoning while effectively reducing redundancy, resulting in more efficient, semantically consistent, and robust multimodal understanding.

III. METHOD

We advance MLLMs for moment retrieval by strengthening temporal perception through the joint integration of audio and visual modalities, coupled with a token compression mechanism to reduce sequence length. The following sections present the overall SMART architecture (§ III-A), describe the audio integration strategy that enhances multimodal understanding (§ III-B), and introduce a shot-aware token compression approach designed to reduce computational cost while preserving fine-grained temporal detail (§ III-C).

A. Pipeline Design

Our model architecture is illustrated in Fig. 2. The model uses two separate branches for visual and audio feature extraction. In the visual branch, EVA-CLIP [28] is adopted as the visual encoder to process sampled frames and produce a sequence of image embeddings, denoted as $\mathbf{V} = [\mathbf{v}_1, \dots, \mathbf{v}_N] \in \mathbf{R}^{N \times P \times D_v}$, where N is the number of frames, P is the number of patches per frame, and D_v is the visual feature dimension. A query-based transformer (Q-Former) then refines each frame embedding to generate frame-level features $\mathbf{V}^q = [\mathbf{v}_1^q, \mathbf{v}_2^q, \dots, \mathbf{v}_N^q] \in \mathbf{R}^{N \times Q \times D_q}$, with Q queries and a Q-Former output dimension of D_q . The output, \mathbf{V}^q , is projected into the LLM feature space via a vision projection layer. The shot-coherent token compression module then reduces token redundancy, producing the final visual representation $\mathbf{V}^L \in \mathbf{R}^{S_v \times D_L}$, where S_v is the number of compressed visual tokens and D_L is the LLM input dimension.

In the audio branch, we adopt BEATs [29], an acoustic tokenizer that produces discrete embeddings rich in semantic information. The audio embeddings are denoted as $\mathbf{A} = [\mathbf{a}_1, \dots, \mathbf{a}_T] \in \mathbf{R}^{T \times D_a}$, where T is the number of audio tokens and D_a is the audio feature dimension. Given the continuous but often redundant nature of audio data, we apply average pooling to reduce the sequence length, followed by an audio projection layer that maps the audio features into the LLM space. The final audio representation is $\mathbf{A}^L \in \mathbf{R}^{S_a \times D_L}$, where S_a is the pooled length of audio tokens.

To construct the input for the language model, we organize a multimodal sequence consisting of time tokens t_i , visual tokens $\mathbf{v}_i^L \in \mathbf{V}^L$, audio tokens $\mathbf{a}_i^L \in \mathbf{A}^L$, a task-specific query q , and a prompt p . To provide explicit temporal context, each time token is placed directly before its corresponding frame embedding. Additionally, to distinguish between modalities, we insert special separator tokens: V_E to mark the end of visual embeddings and A_E for the end of audio embeddings. The resulting multimodal input sequence is structured as:

$$x = [t_1, \mathbf{v}_1^L, t_2, \mathbf{v}_2^L, \dots, V_E, \mathbf{a}_1^L, \mathbf{a}_2^L, \dots, A_E, q, p] \quad (1)$$

This token sequence is then fed into the LLM to identify time segments relevant to the input query q . Inspired by the design of Mr. BLIP [10], the model is prompted to generate a sequence of one or more temporal moments, each represented by a start and end timestamp in seconds. The output follows a nested list format, *e.g.*, $[[s_1, e_1], [s_2, e_2], \dots]$.

B. Audio Integration

Current mainstream benchmark datasets for moment retrieval predominantly contain textual descriptions of visual content. Consequently, prevailing methods tend to rely exclusively on visual cues. However, audio often provides critical complementary information to the visual scene, *e.g.*, footsteps serve as strong acoustic indicators of walking actions. Integrating these acoustic cues enhances query alignment, facilitates cross-modal reasoning, and improves fine-grained temporal localization.

To incorporate audio, we introduce an efficient module that captures semantic acoustic cues and aligns them with

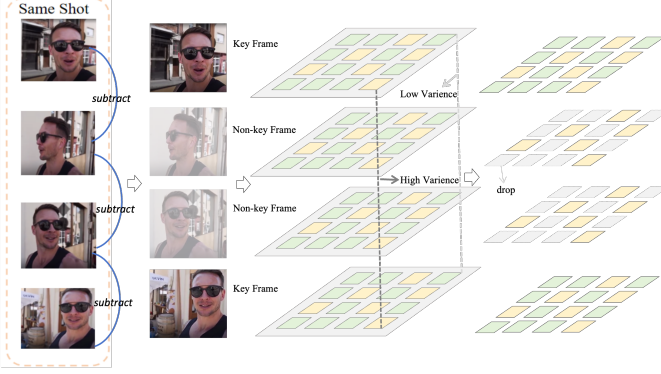


Fig. 3. **Shot-aware token compression:** Key frames are detected via inter-frame differences. Within each shot, high-variance tokens from dynamic regions are preserved, while low-variance tokens from non-key frames are discarded, effectively minimizing redundancy and retaining essential temporal cues for accurate moment retrieval.

the vision-language framework. Raw audio is extracted and resampled to a standardized 16kHz rate, then encoded using the pretrained BEATs [29] model, which is known for its strong semantic understanding of audio signals. To reduce redundancy and maintain computational efficiency, the audio features are temporally pooled into a compact representation and projected to match the visual feature dimension. This design facilitates seamless cross-modal integration, allowing the model to leverage auditory cues (such as speech or environmental sounds) for improved temporal grounding.

Notably, we do not explicitly insert timestamp tokens into the audio features. This is because audio inherently carries dense and continuous temporal structures, which the BEATs encoder captures effectively through its frame-wise encoding and built-in positional embeddings. We further explore and compare different audio integration strategies in the Ablation Study in § IV-C.

C. Shot-aware Token Compression (STC)

We propose the **Shot-aware Token Compression (STC)** strategy to efficiently process long multimodal videos while preserving fine-grained temporal cues. The key insight is that frames within the same shot exhibit strong visual similarity and temporal coherence, introducing redundancy that can be exploited for compression. STC addresses this by (1) identifying keyframes that capture meaningful scene dynamics, and (2) performing intra-shot token compression that removes redundant visual tokens from non-keyframes. This design substantially reduces sequence length while maintaining essential spatio-temporal semantics for accurate moment retrieval. For guiding the compression process, we first segment each video into distinct shots using TransNetV2 [3], which detects shot boundaries based on learned visual transition cues.

Motivation: Dense frame sampling is crucial for capturing subtle visual transitions and transient events, yet it greatly increases sequence length—particularly when combined with audio inputs. Transformer-based LLMs suffer from quadratic self-attention complexity, resulting in high memory cost and degraded inference efficiency for long sequences. Thus, effective token compression is necessary to remove redundancy

while preserving discriminative temporal and semantic information. Existing approaches, such as clustering or pooling [50], [51], often lose fine details in dynamic scenes. In contrast, STC performs compression at the shot level, where intra-shot visual redundancy is high and temporal coherence is preserved, ensuring better efficiency-accuracy trade-offs.

Stage 1 Keyframe Identification: Given visual features \mathbf{F}^v extracted from the image encoder, we compute frame-to-frame differences to detect visually dynamic frames: $\Delta\mathbf{V} = [\Delta\mathbf{v}_1, \dots, \Delta\mathbf{v}_N]$, where each $\Delta\mathbf{v}_i$ encodes patch-wise changes between consecutive frames. The L2 norm of each $\Delta\mathbf{v}_i$ yields a motion magnitude sequence $\mathbf{d} = [d_1, d_2, \dots, d_N]$. To suppress local jitter and noise, we apply a Gaussian filter to obtain a smoothed series $\hat{\mathbf{d}} = \text{Gaussian}(\mathbf{d})$, where each \hat{d}_i represents the smoothed motion magnitude of the i -th frame. Frames with higher \hat{d}_i values are selected as keyframes that contain dynamic content, while the remaining frames are considered non-keyframes with redundant information suitable for compression.

Stage 2 Intra-Shot Token Compression: For each shot, token-level compression is performed within the Q-Former structure, which uses Q learnable queries to encode each frame. Each query captures distinct semantic aspects of the visual content. For all frames in a shot, token variance across the temporal dimension is computed at each query position. High-variance tokens correspond to dynamic elements and are retained across all frames. Low-variance tokens, typically representing static background or redundant content, are discarded from non-keyframes. Their information can be inferred from corresponding tokens in keyframes. This selective compression reduces visual redundancy and computational load, while preserving the temporal fidelity necessary for precise multimodal moment retrieval. The overall STC process is illustrated in Figure 3.

IV. EXPERIMENTAL EVALUATION

A. Experiment Setting

Benchmarks: We validate our model on two widely-used video Moment Retrieval (MR) datasets: (1) **Charades-STA** [1] contains 9,848 videos with an average duration of 30.6 seconds. It provides 16,128 annotations (12,408 for training and 3,720 for testing), where moments average 8.1 seconds in length and queries average 7.22 words. (2) **QVHighlights** [4] consists of 10,148 YouTube videos, each 150 seconds long. Every video includes at least one annotated query (averaging 11.3 words) describing relevant moments, which average 24.6 seconds in duration. The dataset is split into 7,218 training queries and 1,150 validation queries.

Although ActivityNet Captions [45] is widely used for MR, we exclude it from our experiments due to the absence of audio. The official release (“Anet_videos_15fps_short256”) contains only silent videos, making it incompatible with our method, which relies on audio as a complementary modality. Similarly, datasets such as TACoS [54] and MAD [55] provide only pre-extracted visual features, without access to raw video or audio. Since SMART requires frame-level visual

processing, shot detection, and audio encoding, these datasets are unsuitable for our study.

Evaluation Metrics: We evaluate Moment Retrieval (MR) using standard metrics: Recall@K, mean Average Precision (mAP), and mean Intersection over Union (mIoU), computed at specific IoU thresholds. Recall@K measures the proportion of top-K predictions with IoU above a threshold (e.g., R1@0.5). mIoU calculates the average IoU across all predictions, while mAP measures the mean precision across multiple IoU thresholds (e.g., mAP@0.5, mAP@0.75). In summary, R1@0.5 and R1@0.7 assess retrieval accuracy at different IoU levels, mIoU captures average segment overlap, and mAP reflects overall localization precision across thresholds.

Implementation Details: We adopt parameter-efficient fine-tuning with LoRA [44], updating only 0.63% of the model parameters. To mitigate occasional inconsistencies in LLM outputs, we apply lightweight post-processing heuristics to correct minor formatting errors and improve prediction reliability. Training is performed with the AdamW optimizer [2], starting from a learning rate (LR) of 1e-8, linearly warmed up to 3e-4 over the first 10% of iterations, and subsequently decayed with a cosine schedule. During training, frames are randomly sampled from each video.

For Charades-STA, we sample 60 frames per video and train for 30 epochs with a batch size of 16 using 4 GPUs. For QVHighlights, we sample 80 frames per video and train for 30 epochs with a batch size of 32 on 8 GPUs, applying gradient accumulation with a factor of 4. All experiments are conducted on NVIDIA A100 GPUs with 80GB memory.

B. Results

Comparison to the State of the Art: We evaluate our approach on two widely used moment retrieval datasets: *Charades-STA* and *QVHighlights*. As shown in Table I, our model consistently surpasses prior methods across nearly all evaluation metrics on both benchmarks, demonstrating strong generalization regardless of dataset complexity or evaluation scenario.

Our proposed model, **SMART**, achieves substantial performance gains on both datasets, highlighting its robustness across videos ranging in duration from a few seconds to several minutes.

QVHighlights: On the validation set, SMART surpasses previous approaches with improvements of **0.52%** in R1@0.5 and **0.9%** in R1@0.7. On the test set (Table I), SMART establishes new state-of-the-art results across all major metrics, achieving an R1@0.5 of **78.15**, R1@0.7 of **63.16**, mAP@0.5 of **70.76**, and mAP@0.75 of **55.54**. These results represent consistent and notable improvements over the strongest existing baselines, including LLaVA-MR and Mr.BLIPI. Moreover, on the QVHighlights validation set, SMART attains the highest mIoU score of **72.03**, outperforming all competing architectures built on BLIP and CLIP backbones. This demonstrates SMART’s superior ability to model fine-grained temporal alignment and capture multimodal semantics.

Charades-STA: On the Charades-STA test set, SMART also achieves clear performance gains, improving R1@0.5 by **1.61%** and R1@0.7 by **2.59%**. It further attains a new

TABLE I
COMPARISON WITH STATE-OF-THE-ART METHODS ON THE
CHARADES-STA AND QVHIGHLIGHTS DATASETS. **CLIP***: UNLOC [5]
PRETRAINED ON KINETICS 400/700 ACTION CLASSIFICATION, **SF**:
SLOW-FAST BACKBONE.

Method	Backbone	mIoUR1@0.5R1@0.7mAP@0.5mAP@0.75			
		QVHighlights Validation set			
Moment-DETR [4]	SF+CLIP	—	59.68	40.84	—
EaTR [6]	I3D	—	61.36	45.79	61.86
QD-DETR [7]	SF+CLIP	—	62.68	46.66	62.23
UVCOM [12]	SF+CLIP	—	65.10	51.81	—
UnLoc-L [5]	CLIP*	—	66.10	46.70	—
CG-DETR [9]	SF+CLIP	—	67.40	52.10	65.60
R^2 -Tuning [11]	CLIP	—	68.71	52.06	—
VideoLights-B-pt [13]	SF+CLIP+BLIP	—	72.06	57.94	70.38
FlashVTG [14]	SF+CLIP	—	73.10	57.29	72.75
Mr.BLIPI [10]	BLIP-2	—	76.13	63.35	69.39
LLaVA-MR [18]	CLIP+LLM	71.85	78.13	64.13	69.64
SMART	CLIP+LLM	72.03	78.65	65.03	70.46
		QVHighlights Test Set			
SeViLa [56]	BLIP-2	—	54.50	36.50	—
UniVTG [17]	SF+CLIP	—	58.86	40.86	57.60
QD-DETR [7]	SF+CLIP	—	62.40	44.98	62.52
UVCOM [12]	SF+CLIP	—	63.55	47.47	63.37
LMR [15]	SF+CLIP	—	64.40	47.21	64.65
CG-DETR [9]	SF+CLIP	—	65.43	48.38	64.51
R^2 -Tuning [11]	CLIP	—	68.03	49.35	69.04
VideoLights-B-pt [13]	SF+CLIP+BLIP	—	70.36	55.25	69.53
FlashVTG [14]	SF+CLIP	—	70.69	53.96	72.33
Mr.BLIPI [10]	BLIP-2	—	74.77	60.51	68.12
LLaVA-MR [18]	CLIP+LLM	—	76.59	61.48	69.41
SMART	CLIP+LLM	—	78.15	63.16	70.76
		Charades-STA Test set			
Moment-DETR [4]	—	53.63	31.37	—	—
QD-DETR [7]	SF+CLIP	—	57.31	32.55	—
LMR [15]	SF+CLIP	—	55.91	35.19	—
UniVTG [17]	SF+CLIP	50.10	58.01	35.65	—
CG-DETR [9]	SF+CLIP	50.13	58.44	36.34	—
UVCOM [12]	SF+CLIP	—	59.25	36.64	—
R^2 -Tuning [11]	CLIP	—	59.78	37.02	—
UnLoc-L [5]	CLIP*	—	60.80	38.40	—
VideoLights-B-pt [13]	SF+CLIP+BLIP	52.94	61.96	41.05	—
UniMD+Sync [8]	—	—	63.98	44.46	—
InternVideo2-1B [16]	—	—	68.36	45.03	—
EaTR [6]	I3D	—	68.47	44.92	—
Mr.BLIPI [10]	BLIP-2	58.63	69.31	49.29	—
InternVideo2-6B [16]	—	—	70.03	48.95	—
FlashVTG [14]	SF+CLIP	—	70.32	49.87	—
LLaVA-MR [18]	CLIP+LLM	59.78	70.65	49.58	69.96
SMART	CLIP+LLM	61.09	72.26	52.17	69.47
		70.76	55.54	40.43	

best mIoU of **61.09**, outperforming the previous leading method, Mr.BLIPI (58.63), as well as other strong CLIP-based competitors such as CG-DETR and VideoLights-B-pt. These consistent improvements across diverse benchmarks validate the effectiveness of our design choices, particularly the integration of LLM-driven semantic alignment with multimodal supervision. Overall, SMART sets a new state of the art in moment retrieval, demonstrating robust generalization and superior performance across both short- and long-duration video scenarios.

Qualitative Results: Fig. 4 illustrates qualitative comparisons between ground-truth query segments and predicted intervals from baseline MLLM-based models (without audio) and our proposed **SMART**. In Example 1, competing MLLM models fail to maintain temporal precision due to the absence of shot-coherent token compression. In contrast, SMART leverages shot boundaries to retain the most relevant tokens, preserving contextual consistency within each shot and mitigating inter-



Fig. 4. **Qualitative results on QVHighlights [4]:** This figure visualizes the predicted and ground-truth segments for query events. SMART outperforms the visual-text MLLM baseline by preserving shot-level consistency and leveraging audio cues for fine-grained temporal understanding. See text for details.

TABLE II

COMPREHENSIVE ABLATION STUDY OF THE TWO KEY COMPONENTS IN SMART ON THE QVHIGHLIGHTS DATASET. EACH MODULE INDIVIDUALLY IMPROVES PERFORMANCE, WHILE THE FULL MODEL ACHIEVES THE HIGHEST ACCURACY WHEN BOTH COMPONENTS ARE COMBINED.

	Audio	Shot-aware Token Compression	R1@0.5	R1@0.7	mAP@0.5	mAP@0.7
(a)			76.52	63.23	68.99	55.25
(b)	✓		77.23 (+0.71)	64.52 (+1.29)	70.02 (+1.03)	56.66 (+1.41)
(c)		✓	77.03 (+0.51)	63.48 (+0.25)	69.75 (+0.76)	56.27 (+1.02)
(d)	✓	✓	78.65 (+2.13)	65.03 (+1.8)	70.46 (+1.47)	56.72 (+1.47)

ference across shots. Moreover, by incorporating audio cues such as character dialogues, SMART captures fine-grained semantics more effectively, for example in the case of “sharing wired earplug headphones”. These advantages enable SMART to deliver substantially more accurate predictions than competing approaches.

In Example 2, other MLLM-based models incorrectly predict the interval 78s–82s and miss the correct moment around 92s. This misalignment likely results from losing fine-grained visual cues—such as the presence of “two men” during feature compression. In contrast, SMART applies shot-coherent compression that preserves essential information within each shot while filtering redundancy, enabling it to correctly identify the 92s–106s interval, which closely aligns with the ground truth.

In Example 3, for the query “A man talking from a beach”, the keyword talking clearly requires audio understanding. Competing MLLM-based models output a continuous segment from 50s–98s. However, during 88s–96s the man is neither visible nor audible. By incorporating audio cues, SMART detects the absence of speech in that interval and instead predicts two separate segments of 52s–88s and 96s–98s. This matches the ground truth of 52s–88s and 96s–98s much better.

In Example 4, for the query “People are protesting in Armenia against the government”, the ground-truth span multiple intervals of 28s–38s, 62s–72s, and 140s–150s. While scene changes are clear, baseline MLLM models fail to detect the 62s–72s segment. In this portion, the visuals only depict a generic crowd without explicit references to “Armenia”.

However, the background audio includes a reporter explicitly mentioning “Armenia” as the protest location. By leveraging this audio information, SMART captures the missing context and retrieves the correct moments more accurately.

The Appendix provides additional qualitative examples with evaluation and detailed discussions.

C. Ablation Studies

We evaluate the contribution of each component in our framework through ablation studies on QVHighlights (Table II). The baseline (a), which excludes both audio and shot-aware token compression, achieves an R1@0.5 of 76.52 and an mAP@0.5 of 68.99.

Adding the **Audio** component (b) introduces multimodal signals, yielding improvements of **+0.71** in R1@0.5 and **+1.03** in mAP@0.5 over the baseline. Incorporating **Shot-aware Token Compression** (c) enhances temporal consistency, further improving R1@0.5 by **+0.51** and mAP@0.5 by **+0.76**.

Finally, the full **SMART** model (d), which integrates both audio and shot-aware token compression, achieves the best results across all metrics (R1@0.5: **78.65**, R1@0.7: **65.03**, mAP@0.5: **70.46**, mAP@0.7: **56.72**). Notably, this corresponds to a **+2.13** gain in R1@0.5 over the baseline. These results confirm that the proposed components are complementary and jointly enhance multimodal temporal reasoning.

Audio Integration Design: We evaluate various strategies for integrating audio into the prompt on the QVHighlights dataset. As shown in Table III, we compare four approaches: (1) Overall Concatenation, (2) Audio-Visual Fusion, (3) Interleaved Alignment (Frame-Audio Matching), and (4) Voice and Ambient Sound Concatenation.

Among these, (1) **Overall Concatenation**, which directly appends the entire audio sequence after visual features, achieves the best performance with the highest R1@0.5 (**77.23**), R1@0.7 (**64.52**), and mAP@0.5 (**70.02**). This suggests that preserving the full audio context is crucial for accurate moment retrieval. (2) **Audio-Visual Fusion**, which directly merges audio and visual features using cross-attention mechanism, performs poorly. This performance drop may due to the large number of added parameters and insufficient data to learn robust joint representations. (3) **Interleaved Alignment (Frame-Audio Matching)**, which segments audio based on frame sampling, achieves strong mAP@0.5 (70.01) but lower R1@0.5 (76.71), likely due to disruption of audio continuity during segmentation. (4) **Voice and Ambient Sound Concatenation**, which combines voice and ambient audio, performs moderately well (R1@0.5: 76, mAP@0.5: 69.82), but does not outperform Overall Concatenation, indicating that separating voice and ambient sound may reduce coherence. Overall, Overall Concatenation proves to be the best effective strategy, as it retains the global audio context without introducing segmentation noise or forced fusion.

Study of Audio Compression Length L : To evaluate the impact of *audio compression length* L on retrieval performance, we conducted an ablation study on the QVHighlights dataset using only the Overall Concatenation strategy, excluding shot-aware token compression. The aim was to identify the optimal

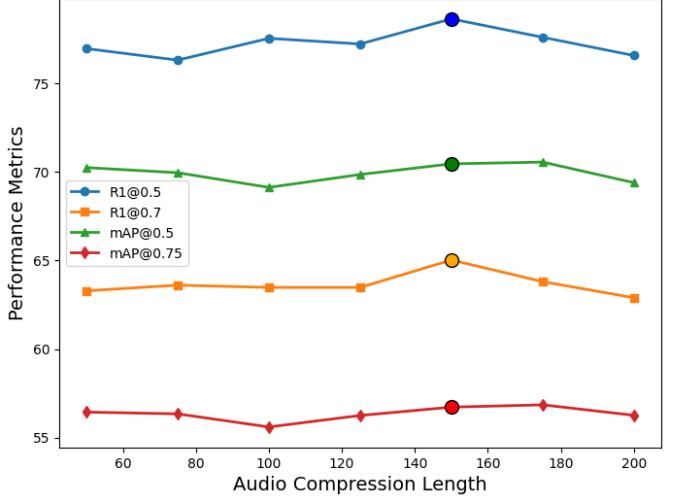


Fig. 5. Impact of **audio compression length** L of the Overall Concatenation strategy on QVHighlights, where the circular marker at $L = 150$ indicates the optimal setting for all metrics.

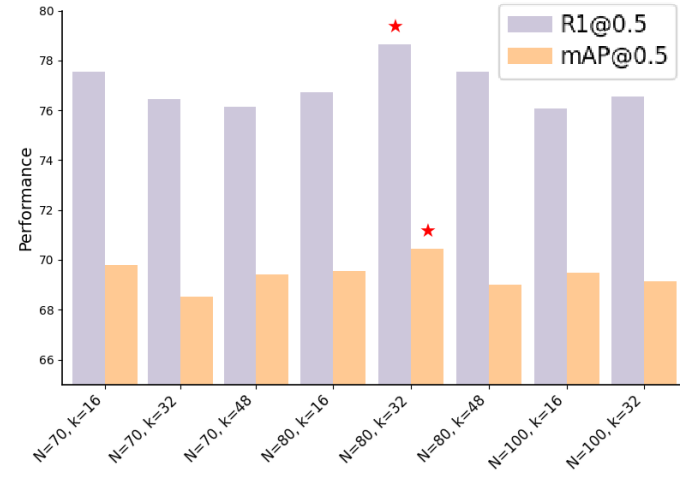


Fig. 6. Determining the optimal **frame number** N and **top- k keyframe** for Shot-aware Token Compression (STC) on QVHighlights, where red stars mark the best configuration ($N = 80$, $k = 32$).

L that balances context preservation with sequence efficiency. Performance was measured by R1@0.5, R1@0.7, mAP@0.5, and mAP@0.75. As shown in Figure 5, $L = 150$ achieves the best overall results, with R1@0.5 of 78.65, R1@0.7 of 65.03, mAP@0.5 of 70.46, and mAP@0.75 of 56.72. Shorter lengths (50 and 75) maintain high precision but lower recall due to limited contextual information, while longer lengths (175 and 200) introduce redundancy and noise, reducing R1@0.7 and mAP@0.5. These findings indicate that $L = 150$ provides the most effective trade-off between context preservation and compression for this strategy.

Study of Frame Number N and Keyframe k for STC: To optimize the Shot-aware Token Compression (STC) module, we conducted a systematic study on QVHighlights. As described in § III-C, STC reduces token redundancy while preserving temporal cues by leveraging shot boundaries and maintaining intra-shot coherence. The module selects key frames with the highest visual changes and compresses low-

TABLE III
ABLATION STUDY OF DIFFERENT AUDIO CONCATENATION STRATEGIES ON THE QVHIGHLIGHTS DATASET.

Audio	R1@0.5	R1@0.7	mAP@0.5	mAP@0.75
Overall Concatenation	77.23	64.52	70.02	56.66
Audio-Visual Fusion	24.84	16.23	20.47	12.26
Interleaved Alignment (Frame-Audio Matching)	76.71	63.16	70.01	56.12
Voice and Ambient Sound Concatenation	76	63.61	69.82	56.83

variance tokens in non-key frames. This ablation study aims to determine the optimal total frame number (N) and number of key frames (k) that balance visual richness with LLM input constraints. As shown in Figure 6, too few key frames ($k = 16$) cause excessive compression and loss of critical visual information, reducing performance (e.g., $N = 70, k = 16$, R1@0.5: 77.55). Too many key frames ($k = 48$) introduce redundancy without consistent gains (e.g., $N = 80, k = 48$, R1@0.5: 77.55). Similarly, increasing N from 70 to 100 captures more visual variation but adds redundancy and sequence length, which can degrade performance (e.g., $N = 100, k = 16$, R1@0.5: 76.06, mAP@0.5: 69.47). Based on these results, the optimal configuration is $N = 80$ frames with $k = 32$ key frames, achieving the best trade-off between visual information richness and sequence efficiency (R1@0.5: 78.65, mAP@0.5: 70.46).

V. CONCLUSION

We introduce **Shot-aware Multimodal Audio-enhanced Retrieval of Temporal Segments (SMART)**, a multimodal moment-retrieval framework that advances temporal reasoning through the integration of audio cues and a **Shot-aware Token Compression** strategy. SMART first detects shot boundaries and computes token-wise variance from Q-Former outputs to selectively retain high-information visual tokens while removing redundant ones. This shot-coherent design preserves intra-shot consistency and critical temporal cues, enabling efficient long-sequence processing without sacrificing precision. In parallel, audio features enrich multimodal representations and enhance semantic grounding. Extensive experiments on Charades-STA and QVHighlights demonstrate that SMART consistently outperforms state-of-the-art methods, particularly for queries requiring fine-grained temporal localization and multimodal comprehension.

Limitations: Despite its strong performance, SMART has limitations. Audio integration is limited to overall embeddings and may miss fine-grained temporal cues in complex scenes. Shot-aware token compression reduces redundancy but can still discard subtle visual details in highly dynamic sequences. Additionally, the framework is trained and evaluated on curated benchmarks, and its generalization to open-world or zero-shot scenarios remains untested.

Future Work: SMART opens multiple avenues for further enhancement. Incorporating dense audio-text alignment could strengthen grounding in complex scenes where audio conveys nuanced information. Extending SMART to open-world or zero-shot retrieval settings would improve generalization to unseen events and diverse domains. Beyond these directions,

integrating additional modalities or hierarchical temporal modeling could further advance robust and scalable multimodal moment retrieval.

REFERENCES

- [1] J. Gao, C. Sun, Z. Yang, and R. Nevatia, “TALL: Temporal activity localization via language query,” in *Proceedings of the IEEE International Conference on Computer Vision (ICCV)*, 2017, pp. 5267–5275.
- [2] I. Loshchilov and F. Hutter, “Decoupled weight decay regularization,” *arXiv:1711.05101*, 2017.
- [3] T. Souček and J. Lokoč, “TransNet V2: An effective deep network architecture for fast shot transition detection,” in *Proc. of the 32nd ACM International Conference on Multimedia (ACM MM)*, pp. 11218–11221, 2024.
- [4] J. Lei, T. L. Berg, and M. Bansal, “Detecting moments and highlights in videos via natural language queries,” *Advances in Neural Information Processing Systems*, vol. 34, pp. 11846–11858, 2021.
- [5] S. Yan, X. Xiong, A. Nagrani, A. Arnab, Z. Wang, W. Ge, D. Ross, and C. Schmid, “UnLoc: A unified framework for video localization tasks,” in *Proceedings of the IEEE/CVF International Conference on Computer Vision (ICCV)*, 2023, pp. 13623–13633.
- [6] J. Jang, J. Park, J. Kim, H. Kwon, and K. Sohn, “Knowing where to focus: Event-aware transformer for video grounding,” in *Proceedings of the IEEE/CVF International Conference on Computer Vision (ICCV)*, 2023, pp. 13846–13856.
- [7] W. Moon, S. Hyun, S. Park, D. Park, and J.-P. Heo, “Query-dependent video representation for moment retrieval and highlight detection,” in *Proceedings of the IEEE/CVF Conference on Computer Vision and Pattern Recognition (CVPR)*, 2023, pp. 23023–23033.
- [8] Y. Zeng, Y. Zhong, C. Feng, and L. Ma, “UniMD: Towards unifying moment retrieval and temporal action detection,” in *European Conference on Computer Vision (ECCV)*, 2024, pp. 286–304.
- [9] W. Moon, S. Hyun, S. Lee, and J.-P. Heo, “Correlation-guided query-dependency calibration for video temporal grounding,” *arXiv:2311.08835*, 2023.
- [10] B. Meinardus, A. Batra, A. Rohrbach, and M. Rohrbach, “The surprising effectiveness of multimodal large language models for video moment retrieval,” *arXiv:2406.18113*, 2024.
- [11] Y. Liu, J. He, W. Li, J. Kim, D. Wei, H. Pfister, and C.-W. Chen, “ R^2 -Tuning: Efficient image-to-video transfer learning for video temporal grounding,” in *European Conference on Computer Vision (ECCV)*, 2024, pp. 421–438.
- [12] Y. Xiao, Z. Luo, Y. Liu, Y. Ma, H. Bian, Y. Ji, Y. Yang, and X. Li, “Bridging the gap: A unified video comprehension framework for moment retrieval and highlight detection,” in *Proceedings of the IEEE/CVF Conference on Computer Vision and Pattern Recognition (CVPR)*, 2024, pp. 18709–18719.
- [13] D. Paul, M. R. Parvez, N. Mohammed, and S. Rahman, “VideoLights: Feature refinement and cross-task alignment transformer for joint video highlight detection and moment retrieval,” *arXiv:2412.01558*, 2024.
- [14] Z. Cao, B. Zhang, H. Du, X. Yu, X. Li, and S. Wang, “FlashVTG: Feature layering and adaptive score handling network for video temporal grounding,” *arXiv:2412.13441*, 2024.
- [15] W. Liu, B. Miao, J. Cao, X. Zhu, B. Liu, M. Nasim, and A. Mian, “Context-enhanced video moment retrieval with large language models,” *arXiv:2405.12540*, 2024.
- [16] Y. Wang *et al.*, “InternVideo2: Scaling foundation models for multimodal video understanding,” in *European Conference on Computer Vision (ECCV)*, 2024, pp. 396–416.
- [17] K. Q. Lin, P. Zhang, J. Chen, S. Pramanick, D. Gao, A. J. Wang, R. Yan, and M. Z. Shou, “UniVTG: Towards unified video-language temporal grounding,” in *Proceedings of the IEEE/CVF International Conference on Computer Vision (ICCV)*, 2023, pp. 2794–2804.

[18] W. Lu, J. Li, A. Yu, M.-C. Chang, S. Ji, and M. Xia, “LLaVAMR: Large language-and-vision assistant for video moment retrieval,” *arXiv:2411.14505*, 2024.

[19] T. Soucek and J. Lokoc, “TransNet V2: An effective deep network architecture for fast shot transition detection,” in *Proceedings of the 32nd ACM International Conference on Multimedia*, 2024, pp. 11218–11221.

[20] L. A. Hendricks, O. Wang, E. Shechtman, J. Sivic, T. Darrell, and B. Russell, “Localizing moments in video with natural language,” in *Proceedings of the IEEE International Conference on Computer Vision (ICCV)*, 2017, pp. 5803–5812.

[21] Y. Yuan, L. Ma, J. Wang, W. Liu, and W. Zhu, “Semantic conditioned dynamic modulation for temporal sentence grounding in videos,” *Advances in Neural Information Processing Systems*, vol. 32, 2019.

[22] D. Zhang, X. Dai, X. Wang, Y.-F. Wang, and L. S. Davis, “MAN: Moment alignment network for natural language moment retrieval via iterative graph adjustment,” in *Proceedings of the IEEE/CVF Conference on Computer Vision and Pattern Recognition (CVPR)*, 2019, pp. 1247–1257.

[23] C. Lea, M. D. Flynn, R. Vidal, A. Reiter, and G. D. Hager, “Temporal convolutional networks for action segmentation and detection,” in *Proceedings of the IEEE/CVF Conference on Computer Vision and Pattern Recognition (CVPR)*, 2017, pp. 156–165.

[24] Y. Zhao, Y. Xiong, L. Wang, Z. Wu, X. Tang, and D. Lin, “Temporal action detection with structured segment networks,” in *Proceedings of the IEEE International Conference on Computer Vision (ICCV)*, 2017, pp. 2914–2923.

[25] R. Zeng, W. Huang, M. Tan, Y. Rong, P. Zhao, J. Huang, and C. Gan, “Graph convolutional networks for temporal action localization,” in *Proceedings of the IEEE International Conference on Computer Vision (ICCV)*, 2019, pp. 7094–7103.

[26] C.-L. Zhang, J. Wu, and Y. Li, “ActionFormer: Localizing moments of actions with transformers,” in *European Conference on Computer Vision (ECCV)*, 2022, pp. 492–510.

[27] Y. Liu, S. Li, Y. Wu, C.-W. Chen, Y. Shan, and X. Qie, “UMT: Unified multi-modal transformers for joint video moment retrieval and highlight detection,” in *Proceedings of the IEEE/CVF Conference on Computer Vision and Pattern Recognition (CVPR)*, 2022, pp. 3042–3051.

[28] Q. Sun, Y. Fang, L. Wu, X. Wang, and Y. Cao, “EVA-CLIP: Improved training techniques for CLIP at scale,” *arXiv:2303.15389*, 2023.

[29] S. Chen, Y. Wu, C. Wang, S. Liu, D. Tompkins, Z. Chen, and F. Wei, “BEATs: Audio pre-training with acoustic tokenizers,” *arXiv:2212.09058*, 2022.

[30] J.-B. Alayrac *et al.*, “Flamingo: A visual language model for few-shot learning,” *Advances in Neural Information Processing Systems*, vol. 35, pp. 23716–23736, 2022.

[31] A. Awadalla *et al.*, “OpenFlamingo: An open-source framework for training large autoregressive vision-language models,” *arXiv:2308.01390*, 2023.

[32] B. Li *et al.*, “Mimic-It: Multi-modal in-context instruction tuning,” *arXiv:2306.05425*, 2023.

[33] R. Zhang *et al.*, “LLaMA-Adapter: Efficient fine-tuning of language models with zero-init attention,” *arXiv:2303.16199*, 2023.

[34] W. Dai *et al.*, “InstructBLIP: Towards general-purpose vision-language models with instruction tuning,” *arXiv:2305.06500*, 2023.

[35] H. Liu, C. Li, Q. Wu, and Y. J. Lee, “Visual instruction tuning,” *arXiv:2304.08485*, 2023.

[36] D. Zhu, J. Chen, X. Shen, X. Li, and M. Elhoseiny, “MiniGPT-4: Enhancing vision-language understanding with advanced large language models,” *arXiv:2304.10592*, 2023.

[37] K. Li *et al.*, “VideoChat: Chat-centric video understanding,” *arXiv:2305.06355*, 2024.

[38] R. Luo *et al.*, “Valley: Video assistant with large language model enhanced ability,” *arXiv:2306.07207*, 2023.

[39] M. Maaaz, H. Rasheed, S. Khan, and F. S. Khan, “Video-ChatGPT: Towards detailed video understanding via large vision and language models,” *arXiv:2306.05424*, 2024.

[40] H. Zhang, X. Li, and L. Bing, “Video-LLaMA: An instruction-tuned audio-visual language model for video understanding,” *arXiv:2306.02858*, 2023.

[41] Z. Cheng *et al.*, “VideoLLaMA 2: Advancing spatial-temporal modeling and audio understanding in video-LLMs,” *arXiv:2406.07476*, 2024.

[42] Y. Su *et al.*, “PandaGPT: One model to instruction-follow them all,” *arXiv:2305.16355*, 2023.

[43] S. Wu, H. Fei, L. Qu, W. Ji, and T.-S. Chua, “NeXT-GPT: Any-to-any multimodal LLM,” in *Proceedings of the International Conference on Machine Learning (ICML)*, 2024, pp. 53366–53397. (PMLR, vol. 235.)

[44] E. J. Hu *et al.*, “LoRA: Low-rank adaptation of large language models,” *arXiv:2106.09685*, 2021.

[45] R. Krishna, K. Hata, F. Ren, L. Fei-Fei, and J. C. Niebles, “Dense-captioning events in videos,” in *Proceedings of the IEEE International Conference on Computer Vision (ICCV)*, 2017, pp. 706–715.

[46] Y. Jin *et al.*, “Efficient multimodal large language models: A survey,” *arXiv:2405.10739*, 2024.

[47] J. Li *et al.*, “A survey on benchmarks of multimodal large language models,” *arXiv:2408.08632*, 2024.

[48] W. Liu, B. Miao, J. Cao, X. Zhu, B. Liu, M. Nasim, and A. Mian, “Context-enhanced video moment retrieval with large language models,” *arXiv:2405.12540*, 2024.

[49] X. Wang, Y. Zhang, O. Zohar, and S. Yeung-Levy, “VideoAgent: Long-form video understanding with large language model as agent,” in *European Conference on Computer Vision (ECCV)*, 2024, pp. 58–76.

[50] S. Zhao, L. Zhu, X. Wang, and Y. Yang, “CenterCLIP: Token clustering for efficient text-video retrieval,” in *Proceedings of the 45th International ACM SIGIR Conference on Research and Development in Information Retrieval*, 2022, pp. 970–981.

[51] B. Clavié, A. Chaffin, and G. Adams, “Reducing the footprint of multi-vector retrieval with minimal performance impact via token pooling,” *arXiv:2409.14683*, 2024.

[52] C. Lin *et al.*, “Fast learning of temporal action proposal via dense boundary generator,” in *Proceedings of the AAAI Conference on Artificial Intelligence*, vol. 34, 2020, pp. 11499–11506.

[53] S. Ji *et al.*, “WavChat: A survey of spoken dialogue models,” *arXiv:2411.13577*, 2024.

[54] A. Rohrbach, M. Rohrbach, W. Qiu, A. Friedrich, M. Pinkal, and B. Schiele, “Coherent multi-sentence video description with variable level of detail,” in *German Conference on Pattern Recognition (GCPR)*, 2014, pp. 184–195.

[55] M. Soldan, A. Pardo, J. L. Alcázar, F. Caba, C. Zhao, S. Giancola, and B. Ghanem, “MAD: A scalable dataset for language grounding in videos from movie audio descriptions,” in *Proceedings of the IEEE/CVF Conference on Computer Vision and Pattern Recognition (CVPR)*, 2022, pp. 5026–5035.

[56] S. Yu, J. Cho, P. Yadav, and M. Bansal, “Self-chained image-language model for video localization and question answering,” *Advances in Neural Information Processing Systems*, vol. 36, pp. 76749–76771, 2023.

[57] X. Zhu, A. K. Elmagarmid, X. Xue, L. Wu, and A. C. Catlin, “InSightVideo: Toward hierarchical video content organization for efficient browsing, summarization and retrieval,” *IEEE Transactions on Multimedia*, vol. 7, no. 4, pp. 648–666, 2005.

[58] C. G. M. Snoek, M. Worring, D. C. Koelma, and A. W. M. Smeulders, “A learned lexicon-driven paradigm for interactive video retrieval,” *IEEE Transactions on Multimedia*, vol. 9, no. 2, pp. 280–292, 2007. ChatGPT said:

[59] T. Chen, W. Wang, Z. Jiang, R. Li, and B. Wang, “Cross-modality knowledge calibration network for video corpus moment retrieval,” *IEEE Transactions on Multimedia*, vol. 26, pp. 3799–3813, 2023.